https://doi.org/10.1038/s41566-019-0363-0

Quantum optical microcombs

Michael Kues [1,2]*, Christian Reimer [3], Joseph M. Lukens [4], William J. Munro [5,6], Andrew M. Weiner [7], David J. Moss [8] and Roberto Morandotti [9,10,11]*

A key challenge for quantum science and technology is to realize large-scale, precisely controllable, practical systems for non-classical secured communications, metrology and, ultimately, meaningful quantum simulation and computation. Optical frequency combs represent a powerful approach towards this goal, as they provide a very high number of temporal and frequency modes that can result in large-scale quantum systems. The generation and control of quantum optical frequency combs will enable a unique, practical and scalable framework for quantum signal and information processing. Here, we review recent progress on the realization of energy–time entangled optical frequency combs and discuss how photonic integration and the use of fibre-optic telecommunications components can enable quantum state control with new functionalities, yielding unprecedented capability.

The generation of large-scale quantum systems that can be precisely controlled is critical[1–3] to enable practical and high-performing devices based on quantum technology that move beyond proof-of-concept demonstrations. These systems can be used for enhancing link speeds in non-classical communications[4], enabling practical quantum-enhanced metrology[5], and for increasing the quantum information content in computations and simulations[6]. Starting from the typical two-dimensional 'qubit' (the quantum analogue of a classical bit) a higher degree of complexity can be achieved through the use of multipartite states (that is, formed by multiple subsystems, such as atoms, electrons or photons and their degrees of freedom) or by increasing the number of quantum dimensions of each party. The Hilbert space size (analogue to the available quantum resource) scales as d^N (with d and N being the number of dimensions and parties, respectively). The polynomial scaling with dimensionality results in a favourable increase in state complexity for smaller dimensions, but becomes less efficient for larger ones, compared with increasing the number of parties. Further, in addition to boosting the quantum information content, complex states may provide a reduced sensitivity to noise — an ever-present challenge for quantum systems — and can enable novel algorithms. For example, two-level 'cluster states' carry unique multipartite entanglement properties that allow the implementation of universal quantum computation via the 'one-way' scheme[7,8], where processing is performed through measurements. Increasing dimensions via high-dimensional subsystems — so-called qudit states — can additionally yield higher noise robustness[9] and allow new algorithms for high-dimensional quantum computation[10].

Developing suitable non-classical systems is, however, pushing the limits of current technology. For example, atomic[11] and superconducting[12] approaches, traditionally based on qubit schemes, need increasingly more technologically complex systems and control methods to increment the number of qubits — a result of their intrinsic physics as well as interactions between neighbours and their environment. For these systems, scaling beyond qubits into qudits is difficult due to their intrinsically shorter decoherence times as well as limited gate fidelities for higher quantum levels.

Photonic systems[13], in contrast, are attractive not only because photons can interact with other quantum systems, can transmit quantum information over long distances and operate at room temperature, but also because photonics can support the generation of very complex quantum states and facilitate their precise control, including high-dimensional systems. Initial approaches based on encoding quantum information on spatial, polarization and orbital angular momentum modes[8,14,15] have been very successful at creating high-dimensional optical states[15,16] as well as qubit cluster states[8,17]. However, despite their success, the footprint of these approaches necessarily grows as the dimensionality increases, due to the spatially distinct nature of the exploited degrees of freedom. This ultimately poses a significant limitation to the degree of complexity that is achievable for practical systems.

The recent introduction of 'quantum frequency combs' can enable the scalable generation of complex (that is, multipartite and high-dimensional) states in the frequency domain[18–22]. Their multimodal characteristics — having many phase-stable frequency modes residing in a single spatial mode — allows these frequency structures to store quantum information in the joint biphoton spectral amplitude and phase, as well as in temporal and frequency correlations. Consequently, quantum frequency combs can store and process a large amount of information in their spectro-temporal quantum modes, quickly becoming a rapidly growing field of research[18–32].

The first quantum frequency combs were based on free-space optical parametric oscillators using nonlinear crystals, where phase-matched parametric down-conversion leads to quantum correlations between frequency modes and results in the generation of so-called squeezed states in a continuous-variable formalism[33,34]. This approach[18,23,24,29–32,35] generates very large-scale photonic quantum systems with mode counts exceeding one million. In synchronously excited systems, this can lead to multimode entangled networks[30,32] that can generate highly complex cluster states[23–26,35,36]. These, however, have proven difficult to control since their very narrow free spectral range (FSR; that is, the frequency mode spacing) of typically only ~100 MHz makes accessing individual modes very challenging, although some reports have achieved state

[1]School of Engineering, University of Glasgow, Glasgow, UK. [2]Department of Engineering, Aarhus University, Aarhus, Denmark. [3]John A. Paulson School of Engineering and Applied Sciences, Harvard University, Cambridge, MA, USA. [4]Quantum Information Science Group, Computational Sciences and Engineering Division, Oak Ridge National Laboratory, Oak Ridge, TN, USA. [5]NTT Basic Research Laboratories and NTT Research Center for Theoretical Quantum Physics, NTT Corporation, Kanagawa, Japan. [6]National Institute of Informatics, Tokyo, Japan. [7]School of Electrical and Computer Engineering and Purdue Quantum Science and Engineering Institute, Purdue University, West Lafayette, IN, USA. [8]Centre for Micro Photonics, Swinburne University of Technology, Hawthorn, Victoria, Australia. [9]Institut National de la Recherche Scientifique (INRS-EMT), Varennes, Quebec, Canada. [10]Institute of Fundamental and Frontier Sciences, University of Electronic Science and Technology of China, Chengdu, China. [11]ITMO University, St Petersburg, Russia. *e-mail: michael.kues@glasgow.ac.uk; morandotti@emt.inrs.ca

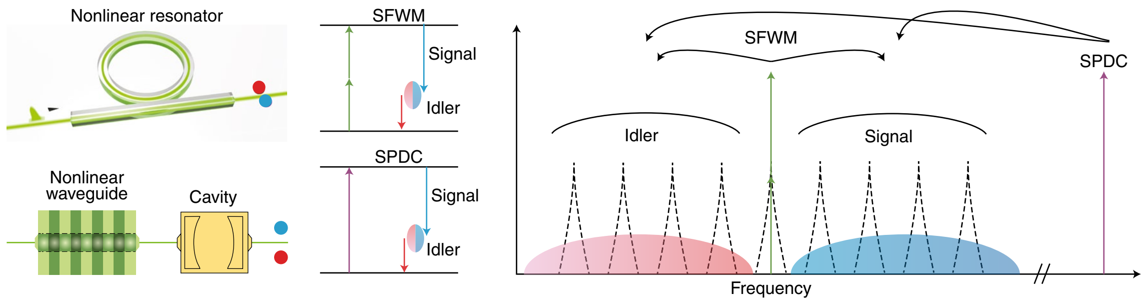

Fig. 1 | Biphoton emission of two correlated photons (called signal and idler) through SPDC or SFWM from filtered nonlinear waveguides or nonlinear resonators. Such approaches lead to discrete energy–time correlated biphoton frequency combs.

characterization using homodyne detection for quantum combs with down to 1 GHz spacing[29]. Consequently, multiple modes are often grouped and manipulated together. Moreover, their large and complex set-ups require sophisticated stabilization schemes, and so these systems are not yet fully suitable for applications outside of the lab. An important distinction between photon and squeezed states is that the latter are Gaussian quantum states[37], and therefore cannot be used for nontrivial quantum information processing in combination with exclusively Gaussian operations and measurements[38–40], such as homodyne detection. To use squeezed states for, for example, quantum computation, non-Gaussian operations and measurements will have to be implemented, such as photon-number-resolving detection. In contrast, entangled photon states combined with coincidence detection can be directly used for quantum information processing.

Integrated photonics is a powerful approach that can allow fundamental advances in scalable classical[41] and quantum[42,43] photonic systems beyond what is achievable using bulk optics. Further, integrated chips that are compatible with the silicon chip industry offer the greatest advantages in terms of being mass-producible, stable, low cost and practical[41,44]. Integrated microcombs, or Kerr combs, in particular, have found substantial interest since their first reports[45–48] about ten years ago, enabling the miniaturization of classical frequency combs[49,50]. Their quantum counterpart — 'quantum microcombs' — operating at the single-photon level, has attracted significant attention in addressing many of the challenges outlined above[19,20,51].

With their unique frequency signature, quantum microcombs can enable photon entanglement in discrete frequency modes that allows for the generation and control of quantum states with considerably enhanced complexity. They achieve this in a scalable, manufacturable platform for generating frequency-multiplexed heralded photons and multiphoton, high-dimensional and hyper-entangled states. This quantum scalability comes from their ability to operate in the frequency picture where more frequency modes and higher dimensions can be easily added to the system without significant overhead or penalty. In contrast to continuous-variable systems, working with discrete-variable photon states is compatible with post-selection using advanced single-photon detection technologies, where losses do not intrinsically degrade the measured quantum state; loss does, however, result in the practical reduction of detection rates. Importantly, quantum photonic systems operating near 1,550 nm also tremendously benefit from, and can build on, well-established telecommunications technology, allowing the realization of chip-/fibre-based quantum devices and distributed fibre quantum networks. Frequency-encoded complex quantum states of light can be readily and directly manipulated using state-of-the-art optical fibre components[20,22,52,53], including filters, routers and modulators. Taken together, all of these factors make quantum microcombs a compelling approach to enabling compact, controllable and scalable complex quantum systems.

Here, we review quantum frequency combs that operate via photon entanglement, beginning with mode-locked quantum frequency combs[28], followed by energy–time entanglement methods, including their generation and control. We focus on integrated optical solutions that operate via the generation of photons using nonlinear optical processes directly in microcavities, as well as via passive spectral filtering following the generation of photons in nonlinear optical waveguides. Finally, we discuss their potential for future applications, addressing the challenges for photonic-based quantum science.

Frequency combs occupied by few photons

Classical frequency combs are characterized by coherently oscillating light fields over many spectral lines, each typically occupied by millions of photons or more. Their strength lies in the phase coherence among the spectral lines achieved via mode-locking approaches, which leads to ultrahigh stability — the basis for applications in metrology, spectroscopy and more. If a classical frequency comb, that is, a pulse train (or more generally any classical coherent light field), is attenuated to the single-photon level, the individual photons keep their spectral phase and temporal pulse shape, which enables, among other applications, their use for quantum communications[54]. More importantly, in addition to this single-photon spectral phase, frequency combs formed by few photons can carry two- or multiphoton spectral phase coherence, which is fundamentally different from single-photon spectral phase coherence. Biphoton phase coherence can occur when two photons are generated from the same process, such as spontaneous parametric down-conversion (SPDC, a second-order nonlinear effect), or spontaneous four-wave mixing (SFWM, a third-order nonlinear effect). In SPDC and SFWM, a nonlinear light–matter interaction mediates the annihilation of one or two photons from an excitation field, simultaneously generating two daughter photons, typically referred to as 'signal' and 'idler' photons. Photons generated via spontaneous parametric nonlinear processes, either directly within a resonator or in a waveguide (and subsequently subjected to periodic spectral filtering), exhibit discrete spectral modes and form a quantum frequency comb (Fig. 1).

The difference between single- and biphoton phase coherence can be understood by considering an analogy to the well-understood single- and biphoton polarization signatures. If a classical linearly polarized light field is attenuated to the single-photon level, the individual photons remain linearly polarized, but if a polarization-entangled photon pair is generated, while the single-photon polarization of each individual photon is random, the biphoton polarization of the state is perfectly defined[55]. In analogy to this, it is possible to generate an energy–time entangled biphoton state where the spectral phases of the individual photons in the state are random, but the two-photon spectral phase is perfectly defined and thus is stable (also referred to as a 'mode-locked two-photon state'[28]).

We first consider the fundamental process that governs the generation of photons via nonlinear optical interactions in non-resonant structures such as waveguides and nanowires. The nonlinear parametric interaction that gives rise to photon pairs preserves the energy, momentum and polarization of the incident optical field, creating two photons in a continuum of temporal and frequency modes. If the phase-matching bandwidth for the process is larger than the excitation field's bandwidth, the joint spectrum and temporal signature of the two photons are correlated. This can be intuitively understood by noting that the spontaneous (that is, non-deterministic) process is effectively simultaneous[56] within the bandwidth limitation of the process (determined by phase matching) that, together with energy conservation, directly leads to time–frequency Einstein–Podolsky–Rosen correlations, enabling one to witness energy–time entanglement directly using uncertainty relations[57]. Energy–time correlated photon pairs have been generated in many ways, including in non-resonant waveguides using quasi-phase-matched periodically poled lithium niobate[57] or silicon waveguides designed, through their geometry, to provide phase matching for SFWM[58], as well as in a range of other integrated devices[43,59–64]. In these cases, the simultaneous generation of two photons immediately dictates that if one photon is detected, the other photon has to arrive at the same time (within the temporal duration of the biphoton), leading to a strong correlation in the two-photon joint temporal intensity (JTI) (Fig. 2a). In addition, this process preserves the energy of the excitation photons. As the photon energy is directly related to the frequency, the sum of the signal and idler frequencies is constant and so energy conservation yields an anti-correlation in the joint spectral intensity (JSI) (Fig. 2b). Indeed, the full quantum state can be described by its joint spectral/temporal amplitude, which also includes phase terms. In the coincidence measurements shown in Fig. 2, only the intensities were measured, while phase coherence could be probed using alternative interferometric techniques, or broadband homodyne detection. In addition to individual measurements of the JTI and JSI[65], it is possible to simultaneously exploit the correlation in time and anti-correlation in frequency, leading to quantum interference in a Franson-type interferometer[66], for example. In particular, if the photons pass through a set of unbalanced interferometers, quantum interference in their coincidences arises that can prove energy–time entanglement of the photon state[66]. Optical interferometers are therefore a common tool to characterize energy–time entangled states. Energy–time entanglement has been demonstrated in systems using a continuous-wave-excited silicon ring resonator where only two single resonator modes were considered[59]. It is customary to characterize this entanglement with the 'Schmidt number', which is the number of significant orthogonal modes derived from a singular value decomposition of the joint spectral amplitude, and which gives a measure of how many frequency–time modes are entangled[67,68].

To achieve discretization in the spectrum, continuous energy–time entangled photons can be generated in a waveguide and then filtered by a cavity, yielding a frequency comb structure. Conversely, rather than filtering the photons after their generation, which leads to high losses in photon flux, it is possible to directly generate photons within a nonlinear resonator[19,28] to avoid filtering losses and at the same time exploit cavity-enhanced parametric processes[69]. This can increase the pair generation efficiency, which is particularly useful for integrated devices as they mainly operate via the less-efficient SFWM process. To enable spectral access to the individual modes, typically achieved via optical filtering, a large mode spacing is advantageous. The use of microresonators as a nonlinear medium is ideal for this, and can be accomplished in a variety of ways, including whispering-gallery-mode resonators in $LiNbO_3$

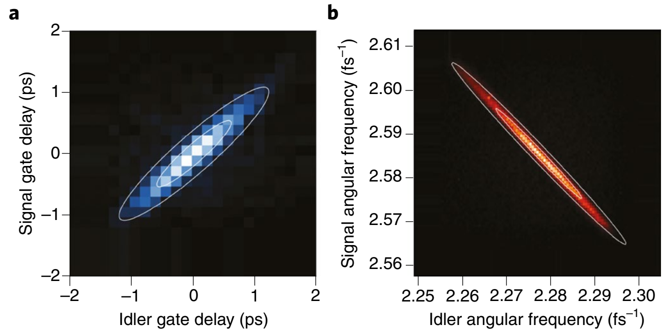

Fig. 2 | Correlation signature of time–energy entangled photons. a,b, JTI (**a**) and JSI (**b**) of an energy–time entangled photon pair. Figure adapted from ref. [65], APS.

(ref. [70]) and integrated ring resonators in a range of platforms such as silicon-on-insulator (SOI)[59,71], Hydex[19,72,73], AlN (ref. [63]) and silicon nitride[20,51]. If the SFWM phase matching is designed so that the bandwidth covers several resonances, which occurs with low anomalous second-order dispersion, it is possible to generate photon pairs over multiple frequency modes[19–21]. Figure 3a shows a typical photon comb spectrum spanning the entire telecommunications band with a 200 GHz frequency spacing, emitted from a silica-doped microring resonator[21]. This large frequency spacing — only achievable with microcavities — allows the use of standard telecom filters (for example, dense wavelength-division multiplexing filters) to select the resonance modes individually for coincidence measurements, for example. Figure 3b depicts a typical correlation matrix resulting from a JSI measurement of the source, showing that coincidences are only detected for frequency components that are symmetrically located with respect to the excitation field[19,20,22,51]. This reflects the energy conservation of the process and thus the quantum frequency comb nature of the generated states. These systems can be directly used as frequency multiplexed heralded single-photon sources (where the idler photon detection indicates the presence of the signal photon)[19], with applications to quantum key distribution[74], for example, or in combination with frequency-shifting schemes for the generation of more deterministic single-photon sources[75,76]. Furthermore, the modes of quantum frequency combs can be utilized as independent sources for multiplexing with wavelength-division multiplexing schemes for entanglement-based quantum communication systems[71].

Looking more closely at the entanglement signature of these emissions, the spectral correlation is no longer continuous but rather exhibits discrete modes (Fig. 3b). The photon lifetime in this case is no longer determined by the bandwidth of the nonlinear process, but by the lifetime of the resonator mode[70,77]. It has been shown that for a cavity-filtered biphoton spectrum, this type of comb structure also manifests itself in quantum interference[27], observed in a Franson interferometer, for example. This leads to the disappearance and reappearance of quantum interference for interferometric imbalances corresponding to multiples of the inverse comb spacing (Fig. 3c)[27,78]. While it is not unexpected that energy–time entanglement between different filtered spectral modes will occur when they are generated by passive filtering of a continuous spectrum, it has not been clear what role the vacuum fluctuations play in photon comb generation when it directly takes place in a nonlinear resonator, and whether energy–time entanglement between spectral modes would still arise in this case. Recent experiments show that energy–time entangled states directly generated in a resonator structure intrinsically cover all frequency modes, which was experimentally confirmed, in a similar fashion, by using optical interferometers with a variable delay[51]. However,

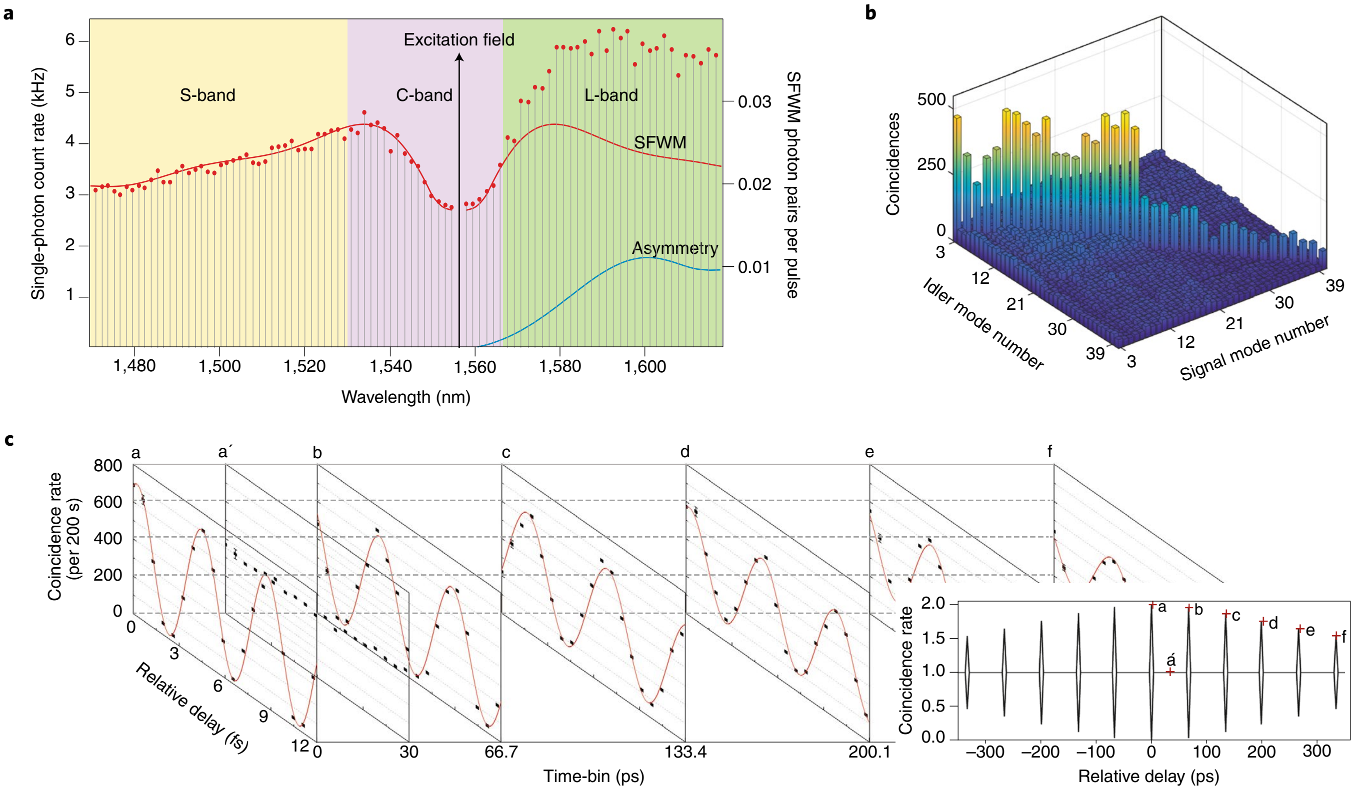

Fig. 3 | Biphoton quantum frequency comb characteristics. **a**, Single-photon spectrum emitted from a microring resonator. **b**, Discrete correlation matrix from a nonlinear ring resonator. **c**, Quantum interference revivals for biphoton combs demonstrating energy–time entanglement covering multiple resonances. a–f indicate temporal positions in the inset. Figure adapted from: **a**, ref. [21], AAAS; **b**, ref. [20], OSA; **c**, ref. [27], Springer Nature Limited.

it is still under debate whether interferometer-based time-domain measurements showing the revival of interference imply that the biphoton phase is stable[27,51].

A deeper understanding of biphoton comb entanglement needs to consider the timescales of the processes relative to both the resonator bandwidths and nonlinear effects taking place. In general, the extent of entanglement between the discrete resonator modes is determined by the overall bandwidth of the nonlinear process and the frequency discretization is often referred to as frequency-bin entanglement[79]. If the excitation field bandwidth is smaller than the resonance bandwidth, the photon emission from a single resonance is multimode in frequency, in which case continuous energy–time entanglement additionally occurs for a single resonance pair. In this case, the Schmidt mode number, which can be quantified through classical seeding experiments or single-photon autocorrelation measurements, is much larger than unity[77,80,81]. In contrast, when the bandwidth of the excitation field is similar to, or larger than, the resonance bandwidth, as is the case for a short-pulsed excitation, energy–time entanglement within a single resonance almost vanishes, yielding a Schmidt mode number close to unity[77]. However, by exciting the system with double or even multiple pulses with delay large enough to display a comb structure within a single resonator linewidth, a discretization in the time domain can be achieved. This excitation can be used to generate photons that additionally have a time-bin entanglement signature[21]. Consequently, multiplexed systems for time-bin and continuous energy–time entanglement have been achieved[71,82].

Complex quantum states generated by microcombs

For many quantum information applications, it is required to have experimental access to all orthogonal modes of the system. Time- and frequency-bin systems are very advantageous in allowing this as their generation and control is readily supported by current laser and modulator technology. Time-bin systems benefit from pulsed lasers and interferometer technologies, whereas frequency-bin systems benefit from telecom filtering and radio-frequency electro-optic spectral mixing. The practical and scalable implementation of time-bin and frequency-bin encoding, particularly when accomplished using microcavities, can lead to the generation of complex quantum states[20–22,52,53] by allowing an increase in the number of state parties (that is, the number of independent subsystems), through more photons or hyper-entangled approaches, and/or by allowing the practical increase of the state dimensionality.

Entangled multiphoton states can be achieved by time-bin encoding of resonator frequency combs. For this, two-photon time-bin entangled states are generated by exciting a nonlinear cavity resonantly matched with two or more laser pulses. The excitation power is kept low enough so that each excitation pulse has a low probability (<0.1) of generating a photon pair, meaning that the photon pair is created in a superposition of the time modes defined by the double pulse. This leads to a time-bin entangled two-dimensional state — that is, an entangled two-qubit state. To characterize and verify the entanglement of this discrete state, projection measurements on the individual temporal modes, as well as their superpositions, are required. This can be obtained by sending signal and idler photons individually through an imbalanced interferometer, where both interferometers have similar arm length mismatches that coincide with the temporal separation of the pump pulses[21]. The indistinguishability between the creation time of the photon pair and which path of the interferometer (the long one or short one) the photons go through, gives rise to quantum interference, that is, a modulation of the coincidence counts when changing the interferometer phase[21]. The interference visibility can be connected to

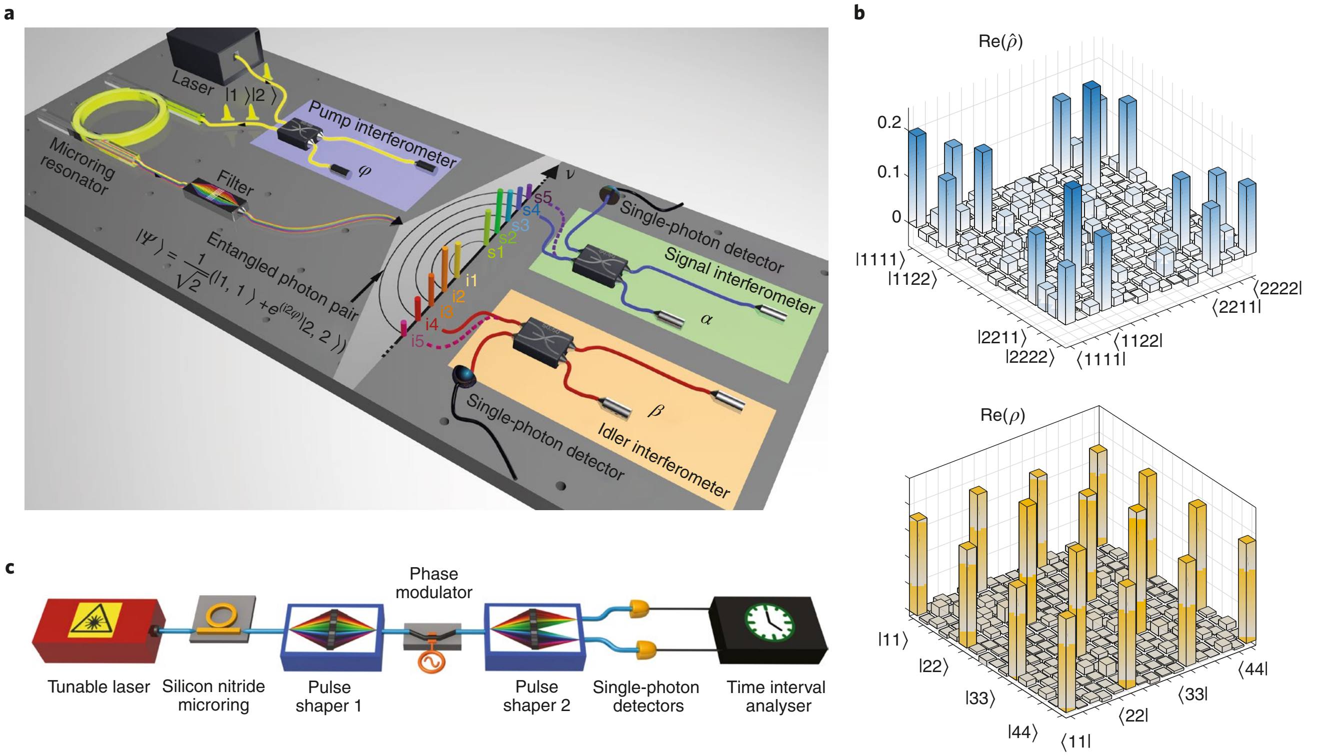

Fig. 4 | Complex quantum states from microring quantum combs. a, Set-up for time-bin multiphoton entangled states generation in frequency combs, where φ, α and β are the interferometer phases, Ψ the quantum state, and i1–i5, s1–s5 the spectral idler and signal components. **b**, Measured density matrix of a four-photon state. **c**, Experimental set-up for the demonstration of frequency-bin entangled high-dimensional states. **d**, Measured density matrix of a four-dimensional state. Figure adapted from: **a**,**b**, ref. [21], AAAS; **c**, ref. [20], OSA; **d**, ref. [22], Springer Nature Limited.

a Bell inequality that, if violated, demonstrates Einstein–Podolsky–Rosen-like correlations and entanglement[66]. Owing to phase matching spanning several resonances of the cavity, time-bin entangled photon pairs can be generated over many resonance pairs simultaneously, leading to a comb of time-bin entangled two-photon states.

The distinctive multimode characteristic of the frequency comb also allows for the generation of four-photon time-bin entangled states. This can be achieved by exploiting two SFWM processes occurring within the coherence time of the pulsed excitation and then post-selecting two signal and idler pairs on different resonances simultaneously. The realization of this four-photon entangled state can be confirmed through quantum interference as well as quantum-state tomography[21] (Fig. 4). Furthermore, it should be possible (by selecting more resonances) to scale to even higher photon numbers of multiphoton states, thereby further increasing the state complexity and Hilbert space size. However, the drawback of multiphoton states is that their detection through post-selection is exponentially reduced by loss as the number of photons increases. A different, and complementary, way to increase the state Hilbert space size while maintaining low photon numbers is to use qudits.

Schemes that make use of the coherence between frequency modes can provide access to high-dimensional entangled states and enable encoding of quantum information on discrete frequency-bin states. Here, the photon pairs are explicitly considered to be in a quantum superposition of many frequency modes[20,22,53]. The experiments that employed interferometers, as discussed above, are not capable of performing projections onto photon states with defined spectral phases within the comb. Furthermore, while broadband single-photon detectors are able to detect photons over a wide frequency band, they are too slow to resolve ultrafast temporal dynamics (on the order of a few picoseconds or less) that result from the phase coherence between different spectral modes. Ultrafast sum-frequency generation, essentially the quantum analogue of intensity autocorrelation methods used extensively in classical ultrafast optics, has been used to resolve the time correlation function of broadband entangled photons with femtosecond resolution[83–88]. However, this approach is limited to local detection (both entangled photons must interact in the same nonlinear crystal), and signal levels are usually too low for use with quantum frequency combs. In the context of squeezed states, broadband detection techniques based on parametric amplification and a nonlinear interferometer configuration have been developed[89,90] to measure the complete joint spectral amplitude in the frequency domain simultaneously across an ultrawide spectrum. However, the feasibility of transferring such techniques to discrete photon states has not been studied yet. To do this, methods to access superpositions of frequency components would be needed.

In analogy to a polarization entangled state, where a single photon can be projected onto specific polarization states by means of phase plates and polarizers, the individual photons of a frequency-bin entangled state need to be projected onto specific spectral phase states. This can be achieved through the use of telecommunications components, many available off-the-shelf such as electro-optic phase modulators (see, for example, Fig. 4c). When driven with a sinusoidal radio-frequency signal, these devices generate sidebands that can be used to superimpose different frequency components of the generated photons. Individual manipulation of the frequency component's phase is possible via programmable optical filters based on optical pulse shaping technology[91], also commonly used in telecom networks. Combining these elements allows one to perform single-photon projections on any arbitrary spectral phase state, and this can be applied to both Bell inequality violations[20,22] as well as quantum state tomography[22] of high-dimensional frequency entangled qudit systems[22] (Fig. 4). Both experiments, using either unbalanced interferometers or employing direct projection measurements with electro-optic modulation, demonstrate that energy–time entanglement covers the full comb. However, the electro-optic modulation approach provides direct access to the quantum modes and their superposition states. Building on this, different arrangements of the control elements (phase modulators, pulse shapers) can enable further quantum processing in the frequency domain, discussed in the next section.

By combining the time- and frequency-bin concepts[53], it is feasible to generate hyper-entangled states that consist of at least four independent parties (qubits or qudits) with only two photons[52]. This becomes possible by using distinct timescales for the frequency- and time-bin entanglements, which enables access to both encoding forms simultaneously.

Multiphoton entanglement[8], high-dimensional states[15] and hyper-entangled[92] states have all predominantly been demonstrated using large-scale free-space optics. Microcavity-based quantum frequency combs, in contrast, can realize these states via integrated chips and/or fibres, which offer enhanced scalability for large-scale quantum states.

Quantum processing with entangled frequency combs

To realize the enormous potential of quantum frequency combs as detailed in the previous section, quantum gates that operate on the frequency degree of freedom are essential. In fact, the very advantages that make quantum frequency combs so attractive as scalable sources — namely their existence in a single spatial mode combined with their immunity to environmental perturbations — require new concepts in controlling them. Whereas path-encoded qubits in the spatial domain can be manipulated with beamsplitters and phase shifters[93,94], frequency-bin encoding demands energy-modifying operations for state manipulation. This is where classical devices from telecommunications, particularly Fourier-transform pulse shapers and electro-optic phase modulators, can play a key role, and indeed they have already had a significant impact on the field of quantum frequency combs[20,22,52,53,79,95–97].

Classical pulse shaping relies on the spectral decomposition of an input light field, followed by the application of a user-defined phase pattern in the generated Fourier plane, either with a fixed mask or liquid-crystal pixels. When the optical frequencies of an input pulse are recombined, the result is an arbitrarily shaped temporal field[91]. However, pulse shapers may also be viewed more generally as user-programmable arbitrary spectral phase and amplitude filters. This provides the capability for manipulating the correlation properties of classical incoherent light fields[98] and, importantly, of quantum light. The time correlation function of entangled photons was first successfully shaped in 2005[83], with subsequent experiments extending to amplitude shaping[84], state characterization[97] and high-dimensional information encoding[85].

Electro-optic phase modulation represents the Fourier counterpart of pulse shaping — it applies a temporal, rather than spectral, phase pattern to the input[99]. Importantly, electro-optic modulation is independent of optical power and is linear in the optical field amplitude, and so it can be efficiently used to manipulate quantum light. Indeed, electro-optic modulation was first demonstrated on single photons in 2008[100], and subsequently applied to continuous energy–time correlations in non-local modulation cancellation[101], frequency-bin entanglement[79] and spread spectral encoding[102]. Recent experiments have also realized frequency shifting[103] and time lensing of single photons[104]. Although these focus on continuous photon spectra, or wavepackets — rather than discrete frequencies — they highlight the importance of electro-optics in single-photon control.

Pulse shaping can be straightforwardly applied to quantum frequency combs — a pulse shaper with sufficient resolution can impart an arbitrary phase shift to each comb line, serving as a bank of phase shifters over all frequency bins. However, inducing interference between frequency bins (analogous to a spatial beamsplitter) is more challenging. As noted in the previous section, electro-optic phase modulators, when driven by a radio-frequency voltage commensurate with the frequency-bin spacing (FSR of the resonator), produce sidebands that allow neighbouring bins to overlap (analogous to a multimode beamsplitter). However, due to the symmetric nature of electro-optic modulation driven by a single tone, any operation designed to interfere adjacent bins also yields unwanted sidebands outside of the modes of interest. Such ‘spectral scattering’ fundamentally limits the success probability of single-modulator-based operations, as is the case in the entanglement-verification schemes described in the previous section[20,22,95] as well as probabilistic frequency-domain Hong–Ou–Mandel interference[105]: they permit projections onto various frequency superpositions, but because of the intrinsic scattering loss, they are not unitary gates in the sense of transforming qubits within a common input–output computational space.

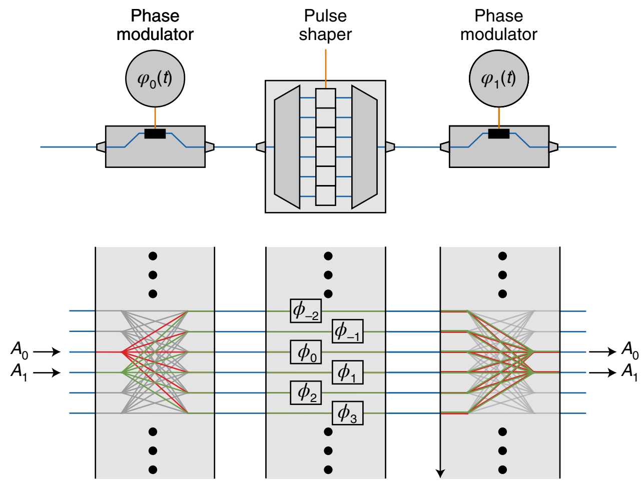

Fig. 5 | Concept of QFP with three elements. The physical configuration (top) comprises phase modulators and a central pulse shaper. The modulators are driven by phase patterns periodic at the frequency-bin spacing, represented by the functions of time $\varphi_0(t)$ and $\varphi_1(t)$, and the pulse shaper applies arbitrary phase shifts to each bin. In the conceptual picture (bottom), frequency bins (rails) are mixed by the modulators and receive specific phase shifts ϕ_n by the pulse shaper. In this example, the cascade ensures probability amplitudes from both modes A_0 (red) and A_1 (green) return to the qubit space on exiting, after experiencing the desired operation.

A solution to this involves cascading phase modulator/pulse shaper pairs. Initially proposed in the context of spectral linear-optical quantum computation[106], the basic idea is to synthesize frequency-bin unitary transformations via a series of temporal and spectral phase operations. These sequences generate probability amplitudes that are initially scattered outside of the encoding space and then caused to return into the encoding space before exiting the gate. This approach was shown to be sufficient to construct a universal gate set[107] consisting of a qubit phase gate, a qubit Hadamard (H) transformation and a two-qubit controlled-Z gate[106]. Scaling arguments imply that any unitary transformation can be achieved in this fashion, with the number of elements increasing only linearly with the dimension of the computational space[106]. In this way, the quantum frequency processor (QFP)[96] forms an alternative unitary decomposition to the more conventional beamsplitter/phase-shifter approach in spatial encoding[93,94]. Figure 5 provides a schematic of how this approach could be applied in a gate for two frequency bins.

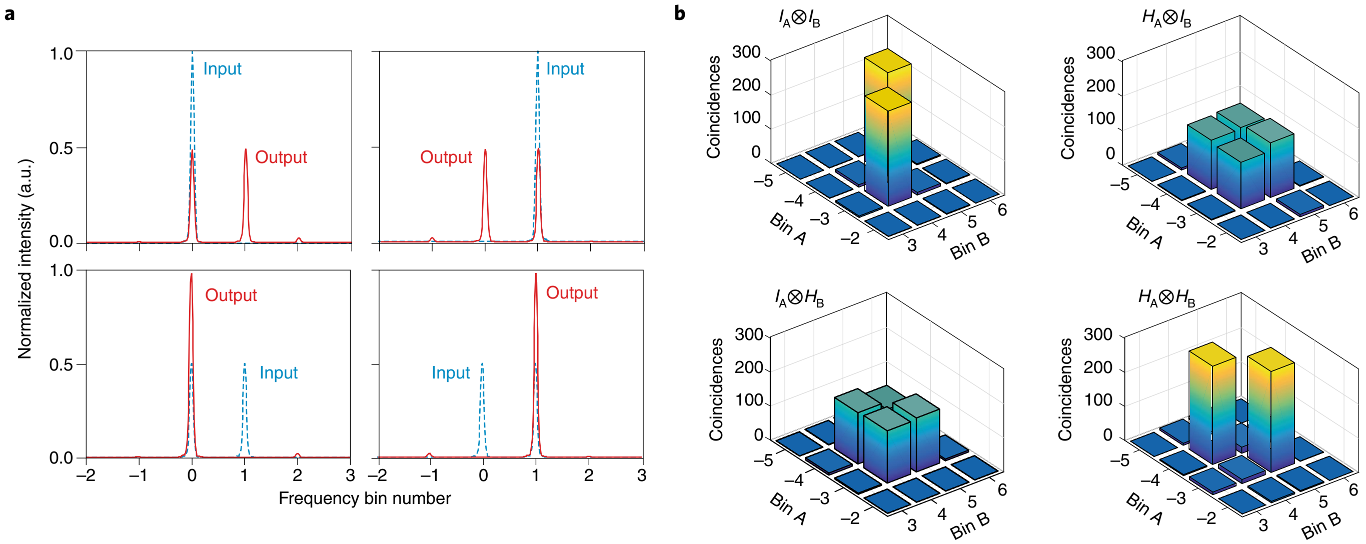

Fig. 6 | Experimental examples of frequency-bin gates. a, Output spectra of a Hadamard gate for the inputs |0⟩ (upper left), |1⟩ (upper right), |0⟩+|1⟩ (lower left) and |0⟩−|1⟩ (lower right). **b**, Measured correlations of a two-qubit frequency-bin entangled state, where each qubit is operated on by either the identity (*I*) or Hadamard (*H*) gates independently. Figure reproduced from: **a**, ref. [108], APS; **b**, ref. [96], OSA.

Although the initial phase modulator spreads the probability amplitudes over bins outside of the two-dimensional input Hilbert space, the subsequent pulse shaper and modulator can reunite the scattered amplitudes via optical interference, yielding a closed single-qubit gate. The effective number of frequency bins populated in the middle of the operation depends on the specific manipulation, but for those examined so far has been on the order of two to four times the size of the computational space[106,108].

QFP gates have recently been demonstrated with the three-element configuration of Fig. 5 designed to synthesize a Hadamard gate (2 × 2 beamsplitter) over two frequency bins. Measured spectra for a 25-GHz-spaced QFP are shown in Fig. 6a[108]. Note that all combinations of bins 0 and 1 produce output states that are also in the qubit computational space, apart from small residual scattering (<3%) due to the use of a pure sinewave phase modulation rather than arbitrary radio-frequency patterns. The measured fidelity is 0.99998 ± 0.00003, confirming the high precision of this approach. Moreover, as noted above, the response of ideal phase modulators yields both upper and lower radio-frequency sidebands, independent of the centre frequency of the input. While this is a challenge in terms of scattering photons into other frequency bins, it turns out to be ideal for parallelization. Specifically, this QFP was found to enable parallel Hadamard gates across the full (40 nm) optical C-band, valuable for accessing the broadband entanglement intrinsic to quantum frequency combs. Extending this approach to higher-dimensional operations is possible as well by, for example, using two-tone radio-frequency drive signals, realizing a frequency-bin tritter (3 × 3 beamsplitter or frequency mixer) in the same QFP[108].

The potential for parallel operations extends beyond the replication of the same gate over many bins — it is also possible to realize different gates on multiple qubits in the same spatial mode. For example, by simply adjusting the pulse shaper phase, the reflectivity of the frequency beamsplitter described above can be smoothly tuned between 50% (which yields the Hadamard gate, *H*) and 0% (which yields the identity operation, *I*). This allows the QFP to operate jointly on spectrally separated qubits with distinct single-qubit gates. Figure 6b provides an example with entangled frequency-bin qubits[96]. When only one qubit experiences the *H* gate, the initial spectral correlations are eliminated. Yet, when both undergo an *H* rotation, correlations are recovered, but with the opposite sign. This suggests the significant potential for performing massively parallelized and arbitrary state rotations on quantum frequency combs. As with any optical approach to quantum information processing, two-photon entangling operations are extremely difficult, and yet the probabilistic designs developed in spatial encoding[94] can be successfully applied to frequency bins, as exemplified in a recent coincidence-basis controlled-NOT (CNOT)[109] gate. Alternatively, by exploiting hyper-entanglement in energy and time, single-photon two-qudit gates have also been realized[52,53]. As the hyperentangled gates are deterministic, they provide, in conjunction with other linear-optical quantum computation approaches, a powerful tool for achieving high-dimensional quantum information processing with entangled frequency combs[52,53].

A key challenge in the QFP paradigm is the bandwidth required of the electro-optic modulators used for phase modulation. Phase modulators have reached ~100 GHz (ref. [110]) with commercial devices being typically limited to 50 GHz. Although using high-order sidebands can extend this bandwidth, such modulation schemes suffer from low efficiency, thus severely limiting the circuit depth (the number of operations that can be concatenated sequentially) as well as qubit (or qudit) connectivity (the maximum separation of frequency bins that can be efficiently mixed by a single modulator). While nonlinear optical processes can support wider bandwidth operation[75,111–114], a more efficient approach is moving to smaller FSR combs[20]. Classical microcombs with FSR spacings below 25 GHz have been reported[115–117] — enabling the coupling of several frequency modes using the fundamental radio-frequency tone of a single electro-optic modulator.

Summary and outlook

Quantum science requires increasingly more complex and large-scale quantum resources, for testing fundamental novel quantum physics as well as realizing relevant and meaningful non-classical signal processing tasks. Solid-state and atom-based quantum systems (for example, trapped ions, superconducting qubits) have been shown to be highly controllable and capable of achieving efficient multiqubit interactions[11,118,119]. Considerable effort has been devoted to scaling up their information content to large quantum systems, but this has proven challenging. Photonic systems, in contrast, while not particularly suited for deterministic two-qubit interactions because of the weak interaction between photons[120], can provide many quantum modes simultaneously in, for example, polarization, path, time and frequency. Furthermore, photons are useful for control, transport and communication in other quantum platforms[121,122], and in fact they are currently the only option for some applications (such as quantum networks). The intrinsic spectral multimode property introduced by quantum frequency combs provides scalability that can compensate in part for the lack of photon interaction efficiency and is thus of significant interest.

The quantum frequency combs reviewed here offer a powerful and versatile platform to generate complex, multimode states in a scalable manner. They provide a unique framework for the manipulation of quantum states in a single spatial mode using standard fibre-optic telecommunications components. While current microcomb-based quantum systems are typically limited to relatively few (~40) frequency modes, and single-photon manipulation schemes to mode counts of three or four, they are scalable by employing smaller FSR resonators and using more advanced low-loss integrated electro-optic modulation[110] and integrated spectral phase manipulation schemes[123,124]. Further research and development in broadband detection techniques for frequency-encoded photon states[83,125] will further advance their use. Quantum photonic integrated circuits will naturally benefit from ongoing advances in classical telecommunications integrated circuits and components, as well as enhanced access to custom designs with the potential for reduced loss through integrated photonics foundry services.

As for all sources of quantum photonic states based on nonlinear spontaneous processes, microcombs are fundamentally stochastic in nature. Efficient quantum photonic systems will benefit from approaches that create effective deterministic sources[81], where quantum frequency combs allow novel approaches that exploit their multimode nature[75]. However, in contrast to previous sources, quantum frequency combs provide a large quantum resource per photon, which could bring the potential to compensate for the drawbacks of non-determinism[52]. Apart from that, the challenges for creating deterministic quantum frequency comb systems are very similar to those of deterministic single-photon sources.

Quantum frequency combs have achieved significant breakthroughs in the generation and control of highly complex photon states that will be critical for large-scale quantum information processing. It is clear that, whichever roles are ultimately assumed by photonic-based quantum information processing, whether it be for interlinks, communications, simulations or computing, those systems will tremendously profit from being able to generate and operate on large-scale multimode quantum states, where microcombs have indeed demonstrated an attractive and powerful approach towards achieving this fundamental goal.

Received: 5 December 2018; Accepted: 17 January 2019;
Published online: 21 February 2019

References

1. Degen, C. L., Reinhard, F. & Cappellaro, P. Quantum sensing. *Rev. Mod. Phys.* **89**, 035002 (2017).
2. Cirac, J. I. & Zoller, P. Goals and opportunities in quantum simulation. *Nat. Phys.* **8**, 264–266 (2012).
3. Ladd, T. D. et al. Quantum computers. *Nature* **464**, 45–53 (2010).
4. Ali-Khan, I., Broadbent, C. J. & Howell, J. C. Large-alphabet quantum key distribution using energy–time entangled bipartite states. *Phys. Rev. Lett.* **98**, 060503 (2007).
5. Lloyd, S. Enhanced sensitivity of photodetection via quantum illumination. *Science* **321**, 1463–1465 (2008).
6. Lanyon, B. P. et al. Simplifying quantum logic using higher-dimensional Hilbert spaces. *Nat. Phys.* **5**, 134–140 (2009).
7. Raussendorf, R. & Briegel, H. J. A one-way quantum computer. *Phys. Rev. Lett.* **86**, 5188–5191 (2001).
8. Walther, P. et al. Experimental one-way quantum computing. *Nature* **434**, 169–176 (2005).
9. Carmichael, H. J., Glauber, R. J. & Scully, M. O. *Direction of Quantum Optics* (Springer, Berlin Heidelberg, 2001).
10. Wang, D.-S., Stephen, D. T. & Raussendorf, R. Qudit quantum computation on matrix product states with global symmetry. *Phys. Rev. A* **95**, 032312 (2017).
11. Blatt, R. & Wineland, D. Entangled states of trapped atomic ions. *Nature* **453**, 1008–1015 (2008).
12. Kandala, A. et al. Hardware-efficient variational quantum eigensolver for small molecules and quantum magnets. *Nature* **549**, 242–246 (2017).
13. O'Brien, J. L., Furusawa, A. & Vučković, J. Photonic quantum technologies. *Nat. Photon.* **3**, 687–695 (2009).
14. Bouwmeester, D., Pan, J.-W., Daniell, M., Weinfurter, H. & Zeilinger, A. Observation of three-photon Greenberger–Horne–Zeilinger entanglement. *Phys. Rev. Lett.* **82**, 1345–1349 (1999).
15. Mair, A., Vaziri, A., Weihs, G. & Zeilinger, A. Entanglement of the orbital angular momentum states of photons. *Nature* **412**, 313–316 (2001).
16. Malik, M. et al. Multi-photon entanglement in high dimensions. *Nat. Photon.* **10**, 248–252 (2016).
17. Prevedel, R. et al. High-speed linear optics quantum computing using active feed-forward. *Nature* **445**, 65–69 (2007).
18. Pinel, O. et al. Generation and characterization of multimode quantum frequency combs. *Phys. Rev. Lett.* **108**, 083601 (2012).
19. Reimer, C. et al. Integrated frequency comb source of heralded single photons. *Opt. Express* **22**, 6535–6546 (2014).
20. Imany, P. et al. 50-GHz-spaced comb of high-dimensional frequency-bin entangled photons from an on-chip silicon nitride microresonator. *Opt. Express* **26**, 1825–1840 (2018).
21. Reimer, C. et al. Generation of multiphoton entangled quantum states by means of integrated frequency combs. *Science* **351**, 1176–1180 (2016).
22. Kues, M. et al. On-chip generation of high-dimensional entangled quantum states and their coherent control. *Nature* **546**, 622–626 (2017).
23. Pysher, M., Miwa, Y., Shahrokhshahi, R., Bloomer, R. & Pfister, O. Parallel generation of quadripartite cluster entanglement in the optical frequency comb. *Phys. Rev. Lett.* **107**, 030505 (2011).
24. Yokoyama, S. et al. Ultra-large-scale continuous-variable cluster states multiplexed in the time domain. *Nat. Photon.* **7**, 982–986 (2013).
25. Menicucci, N. C., Flammia, S. T. & Pfister, O. One-way quantum computing in the optical frequency comb. *Phys. Rev. Lett.* **101**, 130501 (2008).
26. Alexander, R. N. et al. One-way quantum computing with arbitrarily large time-frequency continuous-variable cluster states from a single optical parametric oscillator. *Phys. Rev. A* **94**, 032327 (2016).
27. Xie, Z. et al. Harnessing high-dimensional hyperentanglement through a biphoton frequency comb. *Nat. Photon.* **9**, 536–542 (2015).
28. Lu, Y. J., Campbell, R. L. & Ou, Z. Y. Mode-locked two-photon states. *Phys. Rev. Lett.* **91**, 163602 (2003).
29. Chen, M., Menicucci, N. C. & Pfister, O. Experimental realization of multipartite entanglement of 60 modes of a quantum optical frequency comb. *Phys. Rev. Lett.* **112**, 120505 (2014).
30. Roslund, J., de Araújo, R. M., Jiang, S., Fabre, C. & Treps, N. Wavelength-multiplexed quantum networks with ultrafast frequency combs. *Nat. Photon.* **8**, 109–112 (2014).
31. Gerke, S. et al. Full multipartite entanglement of frequency-comb Gaussian states. *Phys. Rev. Lett.* **114**, 050501 (2015).
32. Cai, Y. et al. Multimode entanglement in reconfigurable graph states using optical frequency combs. *Nat. Commun.* **8**, 15645 (2017).
33. Braunstein, S. L. & van Loock, P. Quantum information with continuous variables. *Rev. Mod. Phys.* **77**, 513–577 (2005).
34. Weedbrook, C. et al. Gaussian quantum information. *Rev. Mod. Phys.* **84**, 621–669 (2012).
35. Yoshikawa, J. et al. Generation of one-million-mode continuous-variable cluster state by unlimited time-domain multiplexing. *APL Photon.* **1**, 060801 (2016).
36. Menicucci, N. C. et al. Universal quantum computation with continuous-variable cluster states. *Phys. Rev. Lett.* **97**, 110501 (2006).
37. Lloyd, S. & Braunstein, S. L. Quantum computation over continuous variables. *Phys. Rev. Lett.* **82**, 1784–1787 (1999).
38. Ohliger, M., Kieling, K. & Eisert, J. Limitations of quantum computing with Gaussian cluster states. *Phys. Rev. A* **82**, 042336 (2010).
39. Lami, L. et al. Gaussian quantum resource theories. *Phys. Rev. A* **98**, 022335 (2018).
40. Niset, J., Fiurášek, J. & Cerf, N. J. No-go theorem for Gaussian quantum error correction. *Phys. Rev. Lett.* **102**, 120501 (2009).
41. Moss, D. J., Morandotti, R., Gaeta, A. L. & Lipson, M. New CMOS-compatible platforms based on silicon nitride and Hydex for nonlinear optics. *Nat. Photon.* **7**, 597–607 (2013).
42. Silverstone, J. W., Bonneau, D., O'Brien, J. L. & Thompson, M. G. Silicon quantum photonics. *IEEE J. Sel. Top. Quantum Electron.* **22**, 390–402 (2016).

43. Tanzilli, S. et al. On the genesis and evolution of integrated quantum optics. *Laser Photon. Rev.* **6**, 115–143 (2012).
44. Hochberg, M. & Baehr-Jones, T. Towards fabless silicon photonics. *Nat. Photon.* **4**, 492–494 (2010).
45. Levy, J. S. et al. CMOS-compatible multiple-wavelength oscillator for on-chip optical interconnects. *Nat. Photon.* **4**, 37–40 (2010).
46. Razzari, L. et al. CMOS-compatible integrated optical hyper-parametric oscillator. *Nat. Photon.* **4**, 41–45 (2010).
47. Del'Haye, P. et al. Optical frequency comb generation from a monolithic microresonator. *Nature* **450**, 1214–1217 (2007).
48. Kippenberg, T. J., Gaeta, A. L., Lipson, M. & Gorodetsky, M. L. Dissipative Kerr solitons in optical microresonators. *Science* **361**, eaan8083 (2018).
49. Stern, B., Ji, X., Okawachi, Y., Gaeta, A. L. & Lipson, M. Battery-operated integrated frequency comb generator. *Nature* **562**, 401–405 (2018).
50. Pasquazi, A. et al. Micro-combs: a novel generation of optical sources. *Phys. Rep.* **729**, 1–81 (2017).
51. Jaramillo-Villegas, J. A. et al. Persistent energy–time entanglement covering multiple resonances of an on-chip biphoton frequency comb. *Optica* **4**, 655–658 (2017).
52. Reimer, C. et al. High-dimensional one-way quantum processing implemented on *d*-level cluster states. *Nat. Phys.* **15**, 148–153 (2019).
53. Imany, P. et al. Deterministic optical quantum logic with multiple high-dimensional degrees of freedom in a single photon. Preprint at https://arxiv.org/abs/1805.04410 (2018).
54. Islam, N. T., Lim, C. C. W., Cahall, C., Kim, J. & Gauthier, D. J. Provably secure and high-rate quantum key distribution with time-bin qudits. *Sci. Adv.* **3**, e1701491 (2017).
55. Kwiat, P. G. et al. New high-intensity source of polarization-entangled photon pairs. *Phys. Rev. Lett.* **75**, 4337–4341 (1995).
56. Hong, C. K. & Mandel, L. Theory of parametric frequency down conversion of light. *Phys. Rev. A* **31**, 2409–2418 (1985).
57. Tanzilli, S. et al. PPLN waveguide for quantum communication. *Eur. Phys. J. D* **18**, 155–160 (2002).
58. Sharping, J. E. et al. Generation of correlated photons in nanoscale silicon waveguides. *Opt. Express* **14**, 12388–12393 (2006).
59. Grassani, D. et al. Micrometer-scale integrated silicon source of time-energy entangled photons. *Optica* **2**, 88–94 (2015).
60. Harris, N. C. et al. Integrated source of spectrally filtered correlated photons for large-scale quantum photonic systems. *Phys. Rev. X* **4**, 041047 (2014).
61. Engin, E. et al. Photon pair generation in a silicon micro-ring resonator with reverse bias enhancement. *Opt. Express* **21**, 27826–27834 (2013).
62. Jin, H. et al. On-chip generation and manipulation of entangled photons based on reconfigurable lithium-niobate waveguide circuits. *Phys. Rev. Lett.* **113**, 103601 (2014).
63. Guo, X. et al. Parametric down-conversion photon-pair source on a nanophotonic chip. *Light Sci. Appl.* **6**, e16249 (2016).
64. Kultavewuti, P. et al. Correlated photon pair generation in AlGaAs nanowaveguides via spontaneous four-wave mixing. *Opt. Express* **24**, 3365–3376 (2016).
65. MacLean, J.-P. W., Donohue, J. M. & Resch, K. J. Direct characterization of ultrafast energy–time entangled photon pairs. *Phys. Rev. Lett.* **120**, 053601 (2018).
66. Franson, J. D. Bell inequality for position and time. *Phys. Rev. Lett.* **62**, 2205–2208 (1989).
67. Law, C. K., Walmsley, I. A. & Eberly, J. H. Continuous frequency entanglement: effective finite Hilbert space and entropy control. *Phys. Rev. Lett.* **84**, 5304–5307 (2000).
68. Christ, A., Laiho, K., Eckstein, A., Cassemiro, K. N. & Silberhorn, C. Probing multimode squeezing with correlation functions. *New J. Phys.* **13**, 033027 (2011).
69. Ou, Z. Y. & Lu, Y. J. Cavity enhanced spontaneous parametric down-conversion for the prolongation of correlation time between conjugate photons. *Phys. Rev. Lett.* **83**, 2556–2559 (1999).
70. Förtsch, M. et al. A versatile source of single photons for quantum information processing. *Nat. Commun.* **4**, 1818 (2013).
71. Mazeas, F. et al. High-quality photonic entanglement for wavelength-multiplexed quantum communication based on a silicon chip. *Opt. Express* **24**, 28731–28738 (2016).
72. Roztocki, P. et al. Practical system for the generation of pulsed quantum frequency combs. *Opt. Express* **25**, 18940–18949 (2017).
73. Reimer, C. et al. Cross-polarized photon-pair generation and bi-chromatically pumped optical parametric oscillation on a chip. *Nat. Commun.* **6**, 8236 (2015).
74. Wang, Q., Zhou, X.-Y. & Guo, G.-C. Realizing the measure-device-independent quantum-key-distribution with passive heralded-single photon sources. *Sci. Rep.* **6**, 35394 (2016).
75. Joshi, C., Farsi, A., Clemmen, S., Ramelow, S. & Gaeta, A. L. Frequency multiplexing for quasi-deterministic heralded single-photon sources. *Nat. Commun.* **9**, 847 (2018).
76. Grimau Puigibert, M. et al. Heralded single photons based on spectral multiplexing and feed-forward control. *Phys. Rev. Lett.* **119**, 083601 (2017).
77. Helt, L. G., Yang, Z., Liscidini, M. & Sipe, J. E. Spontaneous four-wave mixing in microring resonators. *Opt. Lett.* **35**, 3006–3008 (2010).
78. Rambach, M. et al. Hectometer revivals of quantum interference. *Phys. Rev. Lett.* **121**, 093603 (2018).
79. Olislager, L. et al. Frequency-bin entangled photons. *Phys. Rev. A* **82**, 013804 (2010).
80. Silverstone, J. W. et al. Qubit entanglement between ring-resonator photon-pair sources on a silicon chip. *Nat. Commun.* **6**, 7948 (2015).
81. Caspani, L. et al. Integrated sources of photon quantum states based on nonlinear optics. *Light Sci. Appl.* **6**, e17100 (2017).
82. Fang, W.-T. et al. On-chip generation of time-and wavelength-division multiplexed multiple time-bin entanglement. *Opt. Express* **26**, 12912–12921 (2018).
83. Pe'er, A., Dayan, B., Friesem, A. A. & Silberberg, Y. Temporal shaping of entangled photons. *Phys. Rev. Lett.* **94**, 073601 (2005).
84. Zäh, F., Halder, M. & Feurer, T. Amplitude and phase modulation of time–energy entangled two-photon states. *Opt. Express* **16**, 16452–16458 (2008).
85. Lukens, J. M. et al. Orthogonal spectral coding of entangled photons. *Phys. Rev. Lett.* **112**, 133602 (2014).
86. Dayan, B., Pe'er, A., Friesem, A. A. & Silberberg, Y. Nonlinear interactions with an ultrahigh flux of broadband entangled photons. *Phys. Rev. Lett.* **94**, 043602 (2005).
87. O'Donnell, K. A. Observations of dispersion cancellation of entangled photon pairs. *Phys. Rev. Lett.* **106**, 063601 (2011).
88. Lukens, J. M. et al. Generation of biphoton correlation trains through spectral filtering. *Opt. Express* **22**, 9585–9596 (2014).
89. Lemieux, S. et al. Engineering the frequency spectrum of bright squeezed vacuum via group velocity dispersion in an SU(1,1) interferometer. *Phys. Rev. Lett.* **117**, 183601 (2016).
90. Shaked, Y. et al. Lifting the bandwidth limit of optical homodyne measurement with broadband parametric amplification. *Nat. Commun.* **9**, 609 (2018).
91. Weiner, A. M. Femtosecond pulse shaping using spatial light modulators. *Rev. Sci. Instrum.* **71**, 1929–1960 (2000).
92. Kwiat, P. G. Hyper-entangled states. *J. Mod. Opt.* **44**, 2173–2184 (1997).
93. Reck, M., Zeilinger, A., Bernstein, H. J. & Bertani, P. Experimental realization of any discrete unitary operator. *Phys. Rev. Lett.* **73**, 58–61 (1994).
94. Knill, E., Laflamme, R. & Milburn, G. J. A scheme for efficient quantum computation with linear optics. *Nature* **409**, 46–52 (2001).
95. Imany, P., Odele, O. D., Jaramillo-Villegas, J. A., Leaird, D. E. & Weiner, A. M. Characterization of coherent quantum frequency combs using electro-optic phase modulation. *Phys. Rev. A* **97**, 013813 (2018).
96. Lu, H.-H. et al. Quantum interference and correlation control of frequency-bin qubits. *Optica* **5**, 1455–1460 (2018).
97. Bernhard, C., Bessire, B., Feurer, T. & Stefanov, A. Shaping frequency-entangled qudits. *Phys. Rev. A* **88**, 032322 (2013).
98. Binjrajka, V., Chang, C.-C., Emanuel, A. W. R., Leaird, D. E. & Weiner, A. M. Pulse shaping of incoherent light by use of a liquid-crystal modulator array. *Opt. Lett.* **21**, 1756–1758 (1996).
99. Wooten, E. L. et al. A review of lithium niobate modulators for fiber-optic communications systems. *IEEE J. Sel. Top. Quantum Electron.* **6**, 69–82 (2000).
100. Kolchin, P., Belthangady, C., Du, S., Yin, G. Y. & Harris, S. E. Electro-optic modulation of single photons. *Phys. Rev. Lett.* **101**, 103601 (2008).
101. Sensarn, S., Yin, G. Y. & Harris, S. E. Observation of nonlocal modulation with entangled photons. *Phys. Rev. Lett.* **103**, 163601 (2009).
102. Belthangady, C. et al. Hiding single photons with spread spectrum technology. *Phys. Rev. Lett.* **104**, 223601 (2010).
103. Fan, L. et al. Integrated optomechanical single-photon frequency shifter. *Nat. Photon.* **10**, 766–770 (2016).
104. Karpiński, M., Jachura, M., Wright, L. J. & Smith, B. J. Bandwidth manipulation of quantum light by an electro-optic time lens. *Nat. Photon.* **11**, 53–57 (2017).
105. Imany, P. et al. Frequency-domain Hong–Ou–Mandel interference with linear optics. *Opt. Lett.* **43**, 2760–2763 (2018).
106. Lukens, J. M. & Lougovski, P. Frequency-encoded photonic qubits for scalable quantum information processing. *Optica* **4**, 8–16 (2017).
107. Nielsen, M. A. & Chuang, I. L. *Quantum Computation and Quantum Information* (Cambridge University Press, Cambridge, 2010).
108. Lu, H.-H. et al. Electro-optic frequency beam splitters and tritters for high-fidelity photonic quantum information processing. *Phys. Rev. Lett.* **120**, 030502 (2018).
109. Lu, H.-H. et al. A controlled-NOT gate for frequency-bin qubits. *npj Quantum Inf.* https://doi.org/10.1038/s41534-019-0137-z (2019).
110. Wang, C. et al. Integrated lithium niobate electro-optic modulators operating at CMOS-compatible voltages. *Nature* **562**, 101–104 (2018).

111. Tanzilli, S. et al. A photonic quantum information interface. *Nature* **437**, 116–120 (2005).
112. Clark, A. S., Shahnia, S., Collins, M. J., Xiong, C. & Eggleton, B. J. High-efficiency frequency conversion in the single-photon regime. *Opt. Lett.* **38**, 947–949 (2013).
113. Kobayashi, T. et al. Frequency-domain Hong–Ou–Mandel interference. *Nat. Photon.* **10**, 441–444 (2016).
114. Clemmen, S., Farsi, A., Ramelow, S. & Gaeta, A. L. Ramsey interference with single photons. *Phys. Rev. Lett.* **117**, 223601 (2016).
115. Yi, X., Yang, Q.-F., Yang, K. Y., Suh, M.-G. & Vahala, K. Soliton frequency comb at microwave rates in a high-Q silica microresonator. *Optica* **2**, 1078–1085 (2015).
116. Xuan, Y. et al. High-*Q* silicon nitride microresonators exhibiting low-power frequency comb initiation. *Optica* **3**, 1171–1180 (2016).
117. Wang, W.-T. et al. Dissipative Kerr soliton mode-locking and breather states in 19 GHz Si_3N_4 microresonator. In *Conf. Lasers and Electro-Optics* Paper JTh2A.160 (OSA, 2018).
118. Leibfried, D., Blatt, R., Monroe, C. & Wineland, D. Quantum dynamics of single trapped ions. *Rev. Mod. Phys.* **75**, 281–324 (2003).
119. Devoret, M. H. & Schoelkopf, R. J. Superconducting circuits for quantum information: an outlook. *Science* **339**, 1169–1174 (2013).
120. O'Brien, J. L. Optical quantum computing. *Science* **318**, 1567–1570 (2007).
121. Awschalom, D. D., Hanson, R., Wrachtrup, J. & Zhou, B. B. Quantum technologies with optically interfaced solid-state spins. *Nat. Photon.* **12**, 516–527 (2018).
122. Munro, W. J., Azuma, K., Tamaki, K. & Nemoto, K. Inside quantum repeaters. *IEEE J. Sel. Top. Quantum Electron.* **21**, 78–90 (2015).
123. Fontaine, N. K. et al. Compact 10 GHz loopback arrayed-waveguide grating for high-fidelity optical arbitrary waveform generation. *Opt. Lett.* **33**, 1714–1716 (2008).
124. Khan, M. H. et al. Ultrabroad-bandwidth arbitrary radiofrequency waveform generation with a silicon photonic chip-based spectral shaper. *Nat. Photon.* **4**, 117–122 (2010).
125. Karnieli, A. & Arie, A. Frequency domain Stern–Gerlach effect for photonic qubits and qutrits. *Optica* **5**, 1297–1303 (2018).

Acknowledgements

We thank J. Azaña, L. Caspani, P. Roztocki, S. Sciara, Y. Zhang, B. E. Little, S. T. Chu, N. Lingaraju and P. Lougovski for discussions. We acknowledge funding from: Canada Research Chairs (MESI PSR-SIIR); Natural Sciences and Engineering Research Council of Canada (NSERC); H2020 Marie Skłodowska-Curie Actions (MSCA) (656607); ITMO Fellowship and Professorship Program (08-08); 1000 Talents Sichuan Program; Australian Research Council (ARC) (DP150104327); John Templeton Foundation (JTF) number 60478; US Department of Energy, Office of Science, Office of Advanced Scientific Computing Research Quantum Algorithm Teams; Laboratory Directed Research and Development Program of Oak Ridge National Laboratory, managed by UT-Battelle, LLC, for the US Department of Energy; National Science Foundation under award number 1839191-ECCS.

Competing interests

The authors declare no competing interests.

Additional information

Reprints and permissions information is available at www.nature.com/reprints.

Correspondence should be addressed to M.K. or R.M.

Publisher's note: Springer Nature remains neutral with regard to jurisdictional claims in published maps and institutional affiliations.